

## Coupling global chemistry transport models to ECMWF's integrated forecast system

J. Flemming<sup>1</sup>, A. Inness<sup>1</sup>, H. Flentje<sup>4</sup>,  
V. Huijnen<sup>3</sup>, P. Moinat<sup>2</sup>, M.G. Schultz<sup>5</sup>  
and O. Stein<sup>5,6</sup>

Research Department

<sup>1</sup>European Centre for Medium range Weather Forecasting, Reading, United Kingdom

<sup>2</sup>Météo-France, Toulouse, France

<sup>3</sup>Royal Dutch Meteorological Institute, De Bilt, The Netherlands

<sup>4</sup>Deutscher Wetterdienst, Hohenpeissenberg, Germany

<sup>5</sup>Institute of Chemistry and Dynamics of the Geosphere (ICG), FZ Juelich, Germany

<sup>6</sup>Max-Planck-Institute for Meteorology, Hamburg, Germany

May 2009

To be submitted to ACPD

This paper has not been published and should be regarded as an Internal Report from ECMWF.

Permission to quote from it should be obtained from the ECMWF.



European Centre for Medium-Range Weather Forecasts  
Europäisches Zentrum für mittelfristige Wettervorhersage  
Centre européen pour les prévisions météorologiques à moyen

**Series: ECMWF Technical Memoranda**

A full list of ECMWF Publications can be found on our web site under:

<http://www.ecmwf.int/publications/>

Contact: [library@ecmwf.int](mailto:library@ecmwf.int)

**© Copyright 2009**

European Centre for Medium Range Weather Forecasts  
Shinfield Park, Reading, Berkshire RG2 9AX, England

Literary and scientific copyrights belong to ECMWF and are reserved in all countries. This publication is not to be reprinted or translated in whole or in part without the written permission of the Director. Appropriate non-commercial use will normally be granted under the condition that reference is made to ECMWF.

The information within this publication is given in good faith and considered to be true, but ECMWF accepts no liability for error, omission and for loss or damage arising from its use.

## Abstract

The implementation and application of a newly developed coupled system combining ECMWF's integrated forecast system (IFS) with global chemical transport models (CTMs) is presented. The main objective of the coupled system is to enable the IFS to simulate key chemical species without the necessity to invert the complex source and sink processes such as chemical reactions, emission and deposition. Thus satellite observations of atmospheric composition can be assimilated into the IFS using its 4D-VAR algorithm.

In the coupled system, the IFS simulates only the transport of chemical species. The coupled CTM provides to the IFS the concentration tendencies due to emission injection, deposition and chemical conversion. The CTMs maintain their own transport schemes and are fed with meteorological data at hourly resolution from the IFS. The CTM used in the coupled system can be either MOZART-3, TM5 or MOCAGE. The coupling is achieved via the special-purpose OASIS4 software.

The scientific integrity of the coupled system is proven by analysing the difference between stand-alone CTM simulations and the tracer fields in the coupled IFS. The IFS concentration fields match the CTM fields for about 48 hours with the biggest differences occurring in the planetary boundary layer (PBL). The coupled system is a good test bed for process-oriented comparison of the coupled CTM. As an example, the vertical structure of chemical conversion and emission injection is studied for a ten day period over Central Europe for the three CTMs.

The coupled system is validated by comparing daily four-day forecasts with CO and O<sub>3</sub> observation of the Global Atmosphere Watch (GAW) network from Europe, Africa and the Antarctic for the year 2008. Special effort was made to determine the vertical representativeness of the observations. A negative bias for O<sub>3</sub> of about 5-10 ppb and positive bias for CO of up to 20 ppb was detected, which reflects uncertainties in the treatment of emissions, chemistry and deposition in the CTM. The coupled system is able to satisfactorily reproduce the day-to-day variability over the whole forecast length.

## 1. Introduction

Routine exploitation of space-born observations of the atmosphere has been a major contribution to the improvements in numerical weather prediction (NWP) over the last three decades. Inspired by the success of satellite data assimilation in NWP, the "Global and regional Earth-system Monitoring using Satellite and in-situ data" (GEMS) project aims to routinely assimilate satellite observations in order to deliver re-analyses and forecasts of atmospheric composition (Hollingsworth et al., 2008).

The global component of the GEMS system has become part of the integrated forecast system (IFS) of the European Centre for Medium Range Weather Forecast (ECMWF), thereby benefiting from ECMWF's infrastructure for operational satellite data assimilation, weather forecasting and high-performance computing. To enable the IFS, which has until recently been a meteorological model system, to also forecast atmospheric composition, the simulation of emissions, chemical conversion and deposition had to be accounted for. The approach taken for the treatment of reactive gases is presented in this paper.

The forecast and assimilation of global reactive gases are performed by a two-way coupled system, which links the IFS to one of the global chemistry transport models (CTMs), MOCAGE (Josse et al., 2004; Bousserez et al., 2007), MOZART-3 (Kinnison et al., 2007) or TM5 (version KNMI-cy3-GEMS, Krol et al., 2005). Three candidate CTMs were selected because previous model intercomparison studies showed a considerable spread of results. A three-model ensemble can provide some guidance with respect to the robustness of the simulation results. Furthermore, the three candidate CTMs used different coding techniques for parallelisation and more than one option should be available in case of severe performance problems on the ECMWF computer systems. The simulation of global aerosol and greenhouse gases, which have been directly integrated into the IFS source code, is described in Morcrette et al. (2009) and Engelen et al. (2009).

The reactive gas ozone ( $O_3$ ) has been included in global NWP models as a prognostic variable since the mid-1990s. The underlying chemistry schemes focused on stratospheric processes and were often derived from parameterizations of CTM results and climatologies of observations. Geer et al. (2007) compare several linearized schemes for  $O_3$  in respect to their application to satellite data assimilation. At ECMWF,  $O_3$  has been operationally assimilated and forecast using an updated version of the linear stratospheric chemistry scheme by Cariolle and Deque (1986) since 1999 (Hólm et al., 1999), and it was included in the ERA40 re-analysis (Dethof and Hólm, 2004).

The GEMS requirement was to couple the IFS to comprehensive non-linear chemistry schemes for the troposphere and stratosphere. Now completed, the IFS can simulate tropospheric and stratospheric  $O_3$ , carbon monoxide (CO), nitrogen oxides ( $NO_x$ ), formaldehyde (HCHO) and sulphur dioxide ( $SO_2$ ). These species play a key role in atmospheric chemistry and are observable from space (Singh and Jacob, 2000). Examples of the assimilation of these species with the coupled system are given in Inness et al. 2009.

The idea of the coupled system is that the IFS computes only the transport of the reactive gases while the tendencies due to chemical conversion, deposition and emission injection are provided by one of the coupled CTM. The CTM itself is driven by meteorological data which are transferred at high temporal resolution from the IFS to the CTM. For example, the call of a subroutine for chemical conversion in an integrated chemistry-global-circulation-model code is substituted in the coupled system by a call to the coupler software requesting the respective total tendencies from the CTM. The tendencies are then applied to the concentration fields in the IFS at every time step to account for the local concentration changes.

The motivation to build a coupled system, rather than directly integrating the respective modules in the IFS code is elaborated in Section 2.1. Key reasons were the flexibility to apply more than one CTM for the provision of sink and source terms and the reduced development effort.

A potential problem of the coupled approach is that the chemistry and deposition tendencies applied to the IFS concentrations are calculated using the concentration fields that were calculated in the coupled CTM, which uses its own transport, convection and diffusion scheme. The transferred CTM tendencies can therefore be dislocated from the IFS concentration fields to which they are being applied. The dislocation can occur because of (i) the transformation between the CTM and IFS model grids by the coupler software, (ii) the differences between the concentration fields of the CTM and of the IFS due to a different transport simulation, (iii) the coupling interval of one hour being longer than the model time step and (iv) an accumulation of dislocation errors in previous time steps. The dislocation error will be small if the source

and sink tendencies are small in relation to the concentration values, i.e. for long lived species, and if they are small in comparison to the tendencies due to transport processes, i.e. for species with smooth spatial gradients. This paper will show that the IFS concentration fields in the coupled system are scientifically sound and correctly reproduce the simulation results from the CTM.

The remainder of the paper is structured as follows: The system components and different application modes are described in Section 2. Section 0 comprises the test of the scientific integrity of the system, which investigates the impact of dislocation. Also included in this section is a comparison of the vertical structure and magnitude of tendencies due to emission injection and chemical conversion, which helps to give a better understanding of characteristics of the three CTMs.

Finally, in Section 4 near-real-time four-day forecasts by the coupled system IFS-MOZART and additional one-day runs by IFS-TM5 are compared against selected observations from the GAW network ([http://www.wmo.int/pages/prog/arep/gaw/gaw\\_home\\_en.htm](http://www.wmo.int/pages/prog/arep/gaw/gaw_home_en.htm)) in Europe, Africa and the Antarctic for the year 2008. Seasonal biases and the reproduction of the day-to-day variability over the whole forecast length are presented.

## 2. Description of the Coupled System

### 2.1. Motivation for the design of a two-way coupled system

An extension of an earth-system model can follow two approaches: (i) directly integrating subroutines or modules in one unified model or (ii) coupling independent models by means of dedicated coupler software. Direct integration - often referred to as on-line coupling - is normally pursued when complex chemistry schemes are included in meteorological models. Examples of the on-line integration of chemistry modules in weather forecast models are GEM-AQ (Kaminski et al., 2008), GEMS-BACH (Ménard et al., 2007), WRF/Chem (Grell et al., 2005) and ECHAM5-HAMMOZ (Pozzoli et al., 2008 and Rast et al., 2008). Zhang (2008) gives an overview of on-line coupled meteorology and chemistry models with a focus on the modelling of aerosol and cloud-aerosol interactions. An interface standard for the on-line integration of earth-system models which can also include chemistry modules is MESSy (Jockel et al. 2006).

Coupling independent models with coupler software is often applied when the models cover different domains of the earth-system such as ocean and atmosphere. Ford and Riley (2002) present coupler software developed in North America and Europe. An example of the coupled approach in atmospheric chemistry modelling is the CTM MOCAGE which was coupled to the weather forecast model ARPEGE by means of the PALM coupling software (Massart et al., 2005)

A coupled system (IFS-CTM) in which the IFS and a CTM are run in parallel was developed because of the envisaged high development cost to integrate and test complex chemical mechanisms as an integrated part of the IFS. The benefits from using ECMWF's operational data assimilation system and the associated infrastructure for observation processing would be difficult to keep if a new data assimilation system would be build around an existing CTM. Another advantage of the coupled system is the possibility to easily couple different CTMs to the IFS and therefore to be more flexible in the choice of the applied chemistry schemes.

A coupled system of independent components can also better benefit from the ongoing development work of the stand-alone versions of the CTMs since the CTMs stay independent models. Finally, this approach allows for different grid resolutions in the IFS and CTM so that computing resources can be optimally used.

Although designed with the prospect of data assimilation, the coupled system can also be considered as an efficient way to provide meteorological parameters to a CTM at high temporal resolution without the need to access such fields from disk files. Furthermore, it is a research platform to (i) compare the vertical transport schemes of the CTMs and that of the IFS, (ii) to inter-compare the chemical mechanisms of the CTMs by analyzing the tendency field due to chemistry (see Section 3.2) and (iii) to explore the impact of atmospheric composition on numerical weather prediction and its feedback to the tracer concentrations.

## 2.2. Data exchange and experiment setup

The coupled system is a three-dimensional two-way coupled system consisting of the IFS, one of the CTMs MOZART-3, TM5 and MOCAGE and the coupler software OASIS4. In the coupled system, the IFS simulates the advection, vertical diffusion and convection of selected chemical tracers (CO, NO<sub>x</sub>, HCHO, SO<sub>2</sub> and O<sub>3</sub>) and applies tracer tendencies calculated by the coupled CTM to account for sink and source processes such as emission, chemical conversion and deposition. The prognostic tracer variables are also part of the control variables of the data assimilation mode in IFS. Figure 1 shows a schematic of the data flow in the coupled system. Every hour, the IFS provides meteorological fields to drive the CTMs and receives the CTM tendencies. Depending on the mode of operation (see below), concentration fields are exchanged from the IFS to the CTM or vice versa at the start of each coupled run in order to provide the initial conditions for the coupled run. The details of the application and formulation of the tendency terms are given in Section 2.3.

The choice of the exchanged meteorological fields depends on the requirements of the CTM. All CTMs receive fields of humidity, temperature, wind components, or divergence and vorticity in spectral representation, and sensible and latent heat flux. MOZART-3 and MOCAGE simulate their own hydrological cycle whereas TM5 also requires the IFS's precipitation and cloud fields, surface properties and convective mass fluxes.

The experiments with the coupled system are organized as a sequence of several 12 hour runs in data assimilation mode or, in forecast mode, as runs up to four days starting every 24 hours at 0 UTC. In data assimilation mode, the length of the coupled run is given by the length of the 4D-VAR assimilation window, which is normally 12 hours. A more detailed description of how the coupled system is used in data assimilation is given in Inness et. al 2009. In forecast mode, the meteorological fields in the IFS need to be initialized at least every 24 hours with a meteorological analysis in order to avoid a drift from the observed state of the atmosphere.

At the start of each coupled run, the initial conditions of the coupled tracers in the IFS and the CTM are set to the same values: either the CTM fields replace the IFS tracer initial conditions fields (CTM-IC mode) or the IFS tracer fields replace the respective initial conditions of the CTM (IFS-IC mode).

In CTM-IC mode, the CTM gets the whole set of initial conditions from the previous CTM run. In this configuration the concatenated CTM output of IFS-CTM is equivalent to the normal continuous CTM off-line run, except for the higher exchange frequency of meteorological fields.

In IFS-IC mode, CTM fields are used as IFS initial conditions only at the very first coupled run. In all subsequent runs, the IFS's coupled tracers are initialized from the previous IFS run and the respective CTMs fields are replaced by the IFS fields. The un-coupled CTM species are initialised from the previous CTM run as in CTM-IC mode. The IFS-IC mode is applied in data assimilation because the IFS tracer fields contain the assimilated information of the observations. The IFS-IC mode can also be applied to impose vertical tracer profiles simulated by the IFS on the CTM.

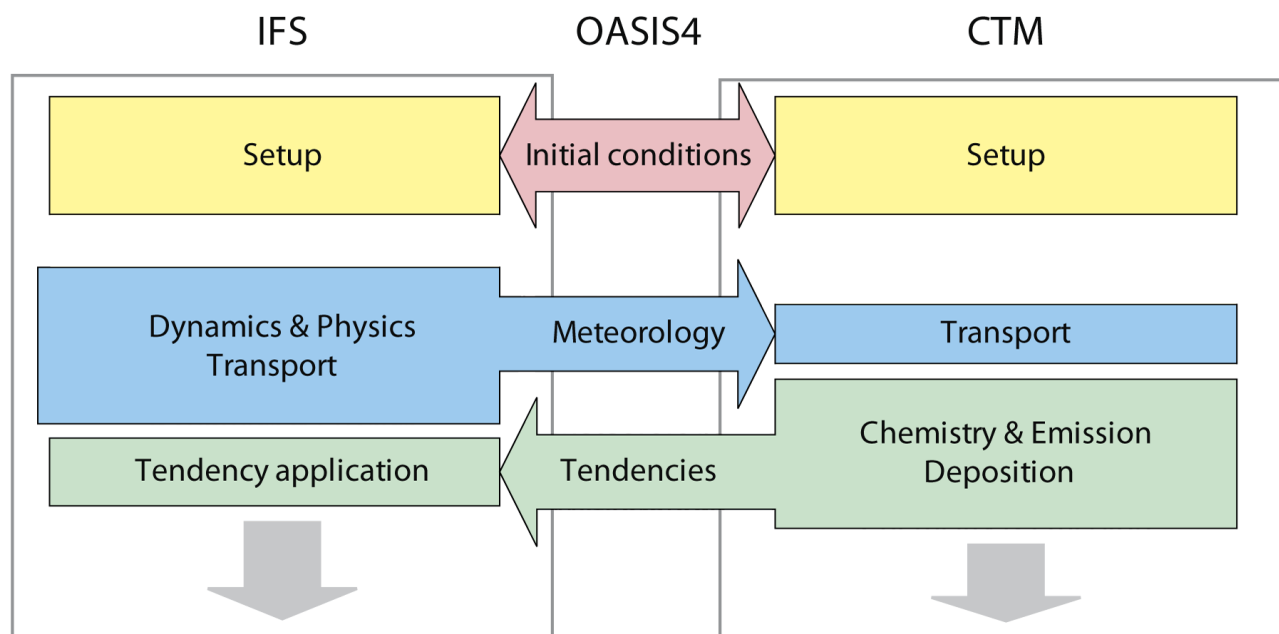


Figure 1 Schematic of the data flow (setup and first time step) in the coupled system consisting of the IFS and a CTM.

### 2.3. Formulation of tendency terms and their application in the IFS

The exchange of concentration tendencies is a unique feature of the coupled system. The formulation of the tendency terms has to reflect (i) operator splitting and time-stepping in both the CTMs and the IFS, (ii) relative size and spatial structure of the tendency fields, and (iii) the computational cost of the exchange.

The CTMs use an operator-splitting approach in which advection, chemistry, emission injection, diffusion and deposition are called in sequence, and the concentrations are updated directly within each operator subroutine. The IFS computes semi-lagrangian advection, diffusion and convection of the tracers based on unperturbed concentration field values from the previous time step (Beljaars et al., 2004) and updates the concentration values with the accumulated tendency of all sink and source processes at the end of the time step.

The total CTM tendencies  $T$  [ $\text{kg kg}^{-1} \text{s}^{-1}$ ] are given by the sum of chemical loss  $L_C$  and production  $P_C$ , production due to emission injection  $P_E$  and loss  $L_D$  due to deposition:

$$T = P_C - L_C + P_E - L_D$$

The injection of surface emissions is integrated in the MOZART-3 diffusion scheme, whereas TM5 and MOCAGE distribute the injected mass in a fixed ratio over selected layers near the surface and apply their diffusion operator after the injection.  $P_E$  is therefore a combination of the emission injection and the tendencies due to vertical turbulent diffusion. Since  $P_E$  already contains the diffusion tendencies, its application in the IFS requires that the IFS diffusion must not be applied again to the respective tracer fields. In order to also use the IFS diffusion scheme for the tracer transport within the coupled system, the effective net surface flux  $\Phi_{E-D}$  from emissions and dry deposition is determined by calculating the total columns of the surface contribution of  $P_E$  and the fraction of  $L_D$  representing dry deposition.  $\Phi_{E-D}$  is then presented as a surface flux to the IFS diffusion scheme and the components  $P_E$  and  $L_D$  are excluded from  $T$  leaving  $T_{Air}$ .

Deposition  $L_D$  and chemical loss  $L_C$  are almost always proportional to the tracer concentration  $x$ . A relative formulation  $L = l x$ , i.e. a loss rate  $l$ , would have linked tendency and concentration values and would have helped to avoid negative concentrations after the application of the CTM tendencies in the IFS. However, it was decided against the relative formulation of tendencies because (i) it would have been more difficult to distinguish chemical loss and production from the output arguments of the chemistry routines, which directly only provide the total change, and (ii) because a separate interpolation of production and loss tendencies, which often almost compensate each other, could have caused imbalances when the two fields are combined again in the IFS.

After consideration of the above arguments, it was decided to transfer and apply the process-specific tendencies of the CTM in one of the following two modes:

1. one three-dimensional tendency field  $T$  containing all sources and sinks as well as diffusion (total-tendency mode)
2. one three-dimensional tendency field  $T_{Air}$  and the effective  $\Phi_{E-D}$  surface flux of emission and deposition (surface-flux mode)

## 2.4. CTM and IFS specifications

In the coupled system, the IFS runs with a T159 spectral resolution and the grid point space is represented by the reduced Gaussian grid (Hortal and Simmons, 1991), which has a grid box size of about 125 km. The CTMs use a regular latitude-longitude grid of about 2° - 3° grid box length. The coupler performs horizontal interpolations for which a bi-linear mode is applied. The IFS runs - for most parts of the globe - at a finer horizontal resolution than the CTMs because this improves (i) the quality of the meteorological forecasts and (ii) the acceptance of high resolution observations within data assimilation mechanism.

The IFS and all CTMs use the same vertical discretization of 60 hybrid sigma-pressure levels, reaching up to 0.1 hPa. The use of an identical vertical structure in the IFS and the CTM avoids the need for vertical interpolation. The minimum coupling interval is 3600 s which is the largest acceptable time step for the IFS at a T159 resolution, and also the time step of some of the CTMs. An overview of the CTM resolution and parameterisations is given in Table 1.

Table 1 Summary of CTM specifications

	<b>MOZART-3</b>	<b>TM5 (KNMI-cy3-GEMS)</b>	<b>MOCAGE</b>
Horizontal resolution	1.875°*1.875°	2°*3°	2°*2°
Vertical resolution	60 layers up to 0.1 hPa	as MOZART-3	as MOZART-3
Meteorological fields	Basic fields, Heat fluxes	as MOZART-3 and precipitation, clouds, convective mass fluxes and surface properties	as MOZART-3
Advection	Flux form semi-lagrangian (Lin and Rood, 1996)	Slopes scheme (Russel and Lerner, 1981)	Semi-implicit, semi-lagrangian (Williamson and Rasch, 1989)
Convection scheme	Hack (1994) for shallow and mid-level convection, Zhang and McFarlane (1995) for deep convection	Tiedtke (1989)	Bechtold et al. (2001), completed by Mari et al. (2000)
Diffusion scheme	Holtslag and Boville (1993)	Holtslag and Moeng (1991) for near surface, Louis (1979) for free troposphere	Louis (1979)
Chemical mechanism	JPL-03 and JPL-06 (Sander et al. 2003, 2006) as described in Kinnison et al. (2007), SO <sub>x</sub> /NH <sub>3</sub> /NH <sub>4</sub> mechanism from MOZART-4 (Emmons et al., in prep.) (115 species, 325 reactions)	CBM4 scheme as described in Houweling et al. (1998) for troposphere, stratospheric O <sub>3</sub> climatology, Fortuin and Kelder (1998) HNO <sub>3</sub> climatology from UARS (55 species, 85 reactions)	REPROBUS (Lefèvre et al., 1994) scheme included in the RACMOBUS scheme (Carslaw et al. 1995) for heterogeneous stratospheric chemistry (118 species and 350 reactions)
Emissions	RETRO (Schultz et al., 2009), GFEDv2 (van der Werft et al. 2006)	as MOZART-3	as MOZART-3

### 3. Scientific integrity of the coupled system

#### 3.1. Comparing IFS concentrations with CTM concentrations

The application of the CTM tendencies to IFS tracers is an approximation because the underlying CTM concentrations could be dislocated from the concentration patterns in the IFS. This dislocation may occur because of (i) the horizontal interpolation from the CTM to the IFS grid and (ii) the differences between the CTM and the IFS transport. In the case of the coupled system, both the IFS and the CTM simulate atmospheric transport processes. Different advection schemes or spatial and temporal resolutions may lead to different concentration fields in the IFS and the CTM.

The most severe consequence of the dislocated tendencies would be negative concentration values in the IFS because of unbalanced loss processes. The severity of the impact of the dislocation depends on the sensitivity of the sink and sources on the concentration itself, i.e. the speed of the chemical conversion and the intensity of the deposition.

In order to minimise the dislocation, the CTM and the IFS concentration fields have to be made as similar as possible by not letting the transport schemes develop different concentration patterns and by periodically aligning the concentration fields in the IFS to the ones in the CTM or vice versa. This aligning is ensured by letting the coupled tracers in the IFS and the CTM start from the same initial conditions (see Section 2.2) either in CTM-IC mode or IFS-IC mode.

The integrity of the coupled system depends on whether the application of external tendency fields accounting for processes not included in the IFS (chemistry, emission and deposition) gives reasonable results for the forecast length. The objective is that the IFS is able to imitate the CTM concentration changes. Therefore, the development of the differences between the IFS tracer fields and their counterpart in the CTM in coupled runs starting from the same MOZART-3 initial conditions was studied. The resemblance of the fields was carefully checked and no unreasonable features in the IFS fields were discovered. The only obvious problem occurred during an earlier attempt to couple  $\text{NO}_2$  rather than  $\text{NO}_x$ . The stratospheric  $\text{NO}$ - $\text{NO}_2$  conversion at sunrise and sunset, which moves around the globe, could not satisfactorily be captured by the coupled system with an exchange frequency of one hour. To avoid this problem, it was decided to use  $\text{NO}_x$  as a coupled species, which did not show the stripe-like undulation as a consequence of the constantly progressing terminator seen in the  $\text{NO}_2$ -fields.

To demonstrate the accuracy of the tendencies application method, Figure 2 shows exemplary time series of spatially averaged  $\text{O}_3$ ,  $\text{CO}$ ,  $\text{HCHO}$  and  $\text{NO}_x$  concentrations from the coupled system IFS-MOZART for model layer 55 (about 240 m above the surface) over Europe. Shown are the two modes of the tendency application (total-tendency and surface-flux mode, see Section 2.3) as well as no tendency application. When no source and sink tendencies were applied the averaged IFS tracer quickly diverged from the CTM reference showing the general need for the tendency application also in a time scale of a few hours. When total tendencies were applied, the IFS could imitate the CTM up to a forecast length of 48 h. The differences were larger, in particular for primary species, when the IFS vertical diffusion scheme injected the effective surface flux  $\Phi_{E-D}$ , indicating a stronger diffusion in the IFS.

To gain a more detailed overview of the ability of the IFS tracers to follow the CTM concentration fields, the relative difference between IFS and CTM fields were calculated for each model grid point and forecast hour in both modes of the tendency application (see Section 2.3). The relative differences were obtained by normalizing with the range, i.e. the difference between maximum and minimum value of the CTM concentration in the respective atmospheric region because it prevents the normalisation with concentration values close to zero. Table 2 contains the percentage of grid points with relative differences lower than 1%, 10% and 100%, discriminating between the PBL, the free troposphere and the stratosphere for the “surface-flux” mode. The differences in “total-tendency” mode were smaller in the PBL because the CTMs diffusion tendencies are directly used in the IFS. The differences were of the same size in the rest of the atmosphere.

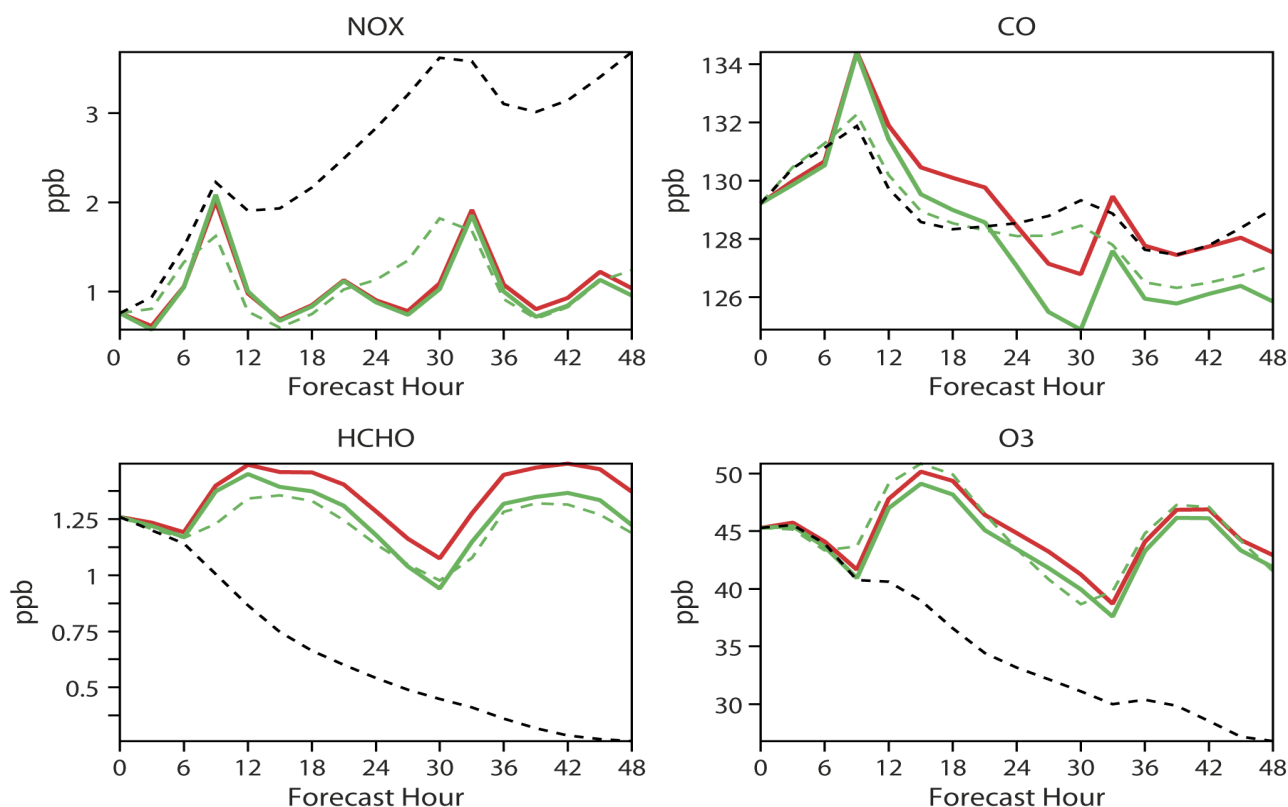


Figure 2: Time series (forecast hour) of the area-averaged  $\text{NO}_x$ ,  $\text{CO}$ ,  $\text{HCHO}$  and  $\text{O}_3$  - concentrations over Europe at about 240 m simulated with the MOZART-3 (red), and simulated with the IFS applying MOZART-3 tendencies in total-tendency mode (green, solid), in surface-flux mode (green-dashed) and no application of tendencies (black, dotted). The coupled IFS tracers simulation (green) imitates that of the CTM MOZART-3 (green) in a satisfactory way.

The discrepancy between the IFS and the CTM coupled tracers developed quickly after the first data exchange and increased from there onwards much more slowly with increasing forecast length. But even after 24 hours the differences were less than 10% at more than 97% of the grid points for every species. When studying the more strict error limit of discrepancies less than 1%, only about 30% of the  $\text{O}_3$  in the PBL could be simulated by the IFS with this accuracy, whereas for the other species 80 - 90% of the grid points satisfied this criterion. The largest absolute differences occurred in the PBL, indicating the high variability in this part of the atmosphere because of emissions injection, diffusion and active chemistry. However, it will be shown in Section 0 that these small differences do not change the errors with respect to observations.

Given the overall uncertainty of the concentration values and the anticipated changes due to data assimilation, it was concluded that IFS concentration fields were scientifically sound since they resembled the CTM fields to a high degree.

Table 2 Fraction of grid points (in %) with relative differences between CTM and IFS value below 1%, 10% and 100% at different forecast lengths for the PBL, the free troposphere and the stratosphere. The run applied the “surface fluxes” mode. The differences have been normalised with the concentration range in the respective area.

Species	Forecast length	PBL			Troposphere			Stratosphere		
		<1%	<10%	<100%	<1%	<10%	<100%	<1%	<10%	<100%
NOX	3	92.7	99.4	100.0	90.9	99.4	100.0	57.0	99.8	100.0
NOX	12	89.5	99.3	100.0	85.6	99.0	100.0	50.1	99.6	100.0
NOX	24	84.3	98.4	100.0	76.2	96.7	99.9	47.2	99.5	100.0
NOX	36	87.1	98.8	100.0	76.2	97.1	100.0	44.5	99.2	100.0
NOX	48	76.4	95.5	99.8	73.1	95.7	99.9	43.3	99.1	100.0
CO	3	96.6	99.9	100.0	94.2	99.9	100.0	84.1	99.9	100.0
CO	12	93.8	99.8	100.0	77.7	99.2	100.0	70.9	99.6	100.0
CO	24	91.0	99.6	100.0	66.8	98.5	100.0	66.1	99.4	100.0
CO	36	90.7	99.7	100.0	62.8	98.0	100.0	59.9	99.0	100.0
CO	48	88.2	99.6	100.0	60.0	97.7	100.0	57.7	98.8	100.0
HCHO	3	93.5	99.9	100.0	88.9	99.3	100.0	57.9	96.3	99.9
HCHO	12	86.1	99.5	100.0	73.9	96.6	100.0	50.4	94.6	99.6
HCHO	24	81.3	99.2	100.0	62.7	92.9	100.0	49.4	94.2	99.7
HCHO	36	81.6	99.2	100.0	64.2	93.7	100.0	45.8	93.1	99.5
HCHO	48	78.3	99.1	100.0	54.4	90.3	100.0	45.1	93.7	99.6
O3	3	69.5	99.4	100.0	81.0	99.8	100.0	80.2	100.0	100.0
O3	12	38.4	97.9	100.0	51.6	97.9	100.0	67.0	99.9	100.0
O3	24	30.6	97.1	100.0	40.4	96.6	100.0	60.4	99.8	100.0
O3	36	24.4	95.7	100.0	35.2	95.4	100.0	55.2	99.7	100.0
O3	48	24.7	96.7	100.0	32.0	94.5	100.0	51.9	99.5	100.0
SO2	3	97.3	99.9	100.0	96.4	99.7	100.0	97.4	99.7	100.0
SO2	12	95.5	99.7	100.0	91.0	98.8	100.0	92.0	98.8	100.0
SO2	24	93.4	99.4	100.0	88.6	98.3	99.9	88.6	98.4	99.9
SO2	36	93.8	99.5	100.0	83.1	96.8	99.9	83.1	96.8	99.9
SO2	48	92.2	99.2	100.0	82.1	96.6	99.9	83.0	96.6	100.0

### 3.2. Model diagnostics based on the tendency terms

Studying the source and sink tendencies from the emission injection and chemical conversion may help to gain more insight into the CTMs. In a case study, the tendency terms from the different source and sink processes were analysed with emphasis on the troposphere over all 287 land points in Central Europe (42N/-10W - 55N/10E) for a ten day period in June 2004.

Vertical profiles of the area-averaged concentration changes from each CTM were calculated for day (12 UTC) and night conditions (0 UTC) were calculated and, for display, normalised with the area-averaged concentrations. The “chemistry” profile includes the net chemical conversion and the negligible contributions from wet deposition and air-borne emissions ( $T_{Air}$ , see 2.3.) The “emission” profile comprises the three-dimensional tendencies due to emission injection, diffusion, convection and dry deposition, whose total columns were used to calculate the net surface flux  $\Phi_{E-D}$  in “surface-flux” mode. The sum of the two is equal to  $T$  in total-tendency mode.

The CO tendencies for emission injection and diffusion (Figure 3, left) during the day showed that diffusion, despite CO emissions, leads to a concentration decrease close to the surface and an accumulation in the upper part of the boundary layer. The accumulation zone in MOZART-3 was largely confined to 900 hPa whereas the vertical transport in TM5 and MOCAGE reached higher levels, indicating more pronounced diffusion and convection. The stable conditions during the night caused increasing CO concentration values only in the lowest two to three model levels in all CTMs. The chemical conversion of CO (Figure 3, right) is linked to daytime photochemistry, which explains the absence of concentration changes during the night for all models. The relative concentration changes due to chemistry were smaller than the changes due to emissions and diffusion. However, chemical CO loss occurred throughout the vertical column of the troposphere. All models simulated the CO depletion due to oxidation with OH in the free troposphere. In spite of similar formulations of the chemical rate constant for CO oxidation, the relative chemical tendency of CO among the three CTMs differs by more than a factor of two. MOCAGE showed the strongest chemical loss both in relative and absolute terms. A comparison of the OH concentrations of the three CTMs confirmed that MOCAGE’s average OH concentrations were higher by about 0.05 ppt than TM5 and by 0.07 ppt than MOZART-3. The CTMs simulated a net chemical production of CO due to oxidation of volatile organic compounds in the PBL, which was smallest in TM5 and largest in MOZART-3.

The vertical profile of the surface flux related tendencies for  $\text{NO}_x$  resembled that of CO although the relative changes were about ten times larger (Figure 4, left). The mixing of the emissions during the day was again limited to a shallower layer in MOZART-3 compared to the other CTMs. The chemistry (Figure 4, right) caused a loss of  $\text{NO}_x$  in the lower troposphere of up to 40% per hour during the day because of conversion into  $\text{HNO}_3$  and PAN. Again MOCAGE simulated the strongest tropospheric  $\text{NO}_x$  depletion during the day because of the higher OH concentrations. During the night, only TM5 and MOZART-3 computed tropospheric  $\text{NO}_x$  loss, in the range of 10%, probably due to the heterogeneous  $\text{N}_2\text{O}_5$  uptake on clouds and aerosols, which is not included in MOCAGE.

The  $\text{O}_3$  surface flux (Figure 5, left) is caused by dry deposition at the surface. Compared to this large loss, the averaged diffusion did not contribute substantially to a systematic vertical concentration change in any of the CTMs. During the day,  $\text{O}_3$  production occurred in the PBL of all CTMs, and  $\text{O}_3$  loss occurred in the lowest layer during the night because of titration with NO, which was concentrated there. The comparatively low  $\text{O}_3$  loss can be attributed to the fact that most of the titration took place before midnight. Only TM5 simulated reduced  $\text{O}_3$  production in the lowest layer during the day, which was probably related to the high  $\text{NO}_x$  increase there.

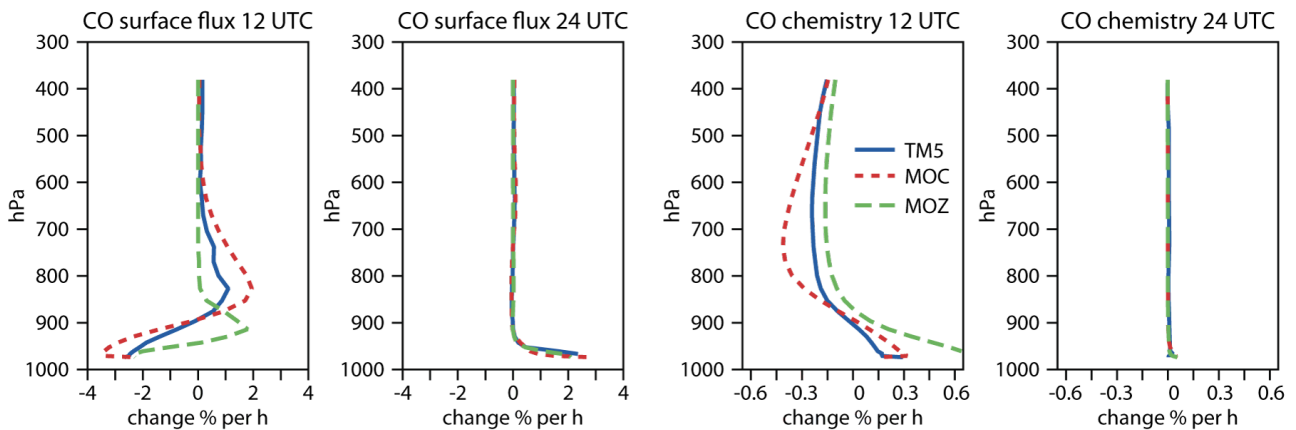


Figure 3 Profile of the area averaged (over Europe) relative changes per hour in percent of CO due to emissions injection and deposition (left two panels) and due to chemistry (right two panels) from TM5, MOZART-3 (MOZ) and MOCAGE (MOC) at 12 and 24 UTC.

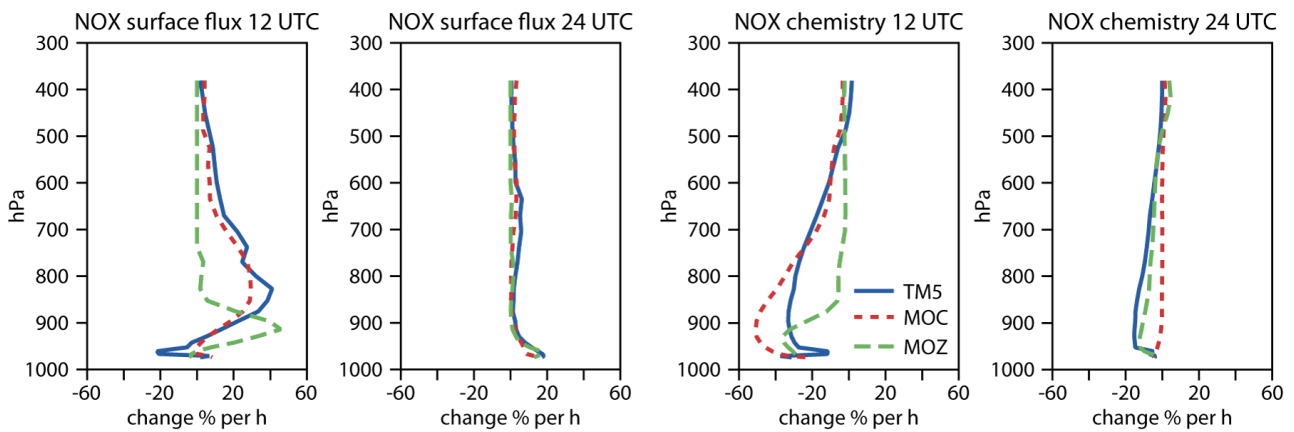


Figure 4 Profile of the area averaged (over Europe) relative changes per hour in percent of NO<sub>x</sub> due to chemistry and due to emissions injection and deposition from TM5, MOZART-3 (MOZ) and MOCAGE (MOC) at 12 and 24 UTC.

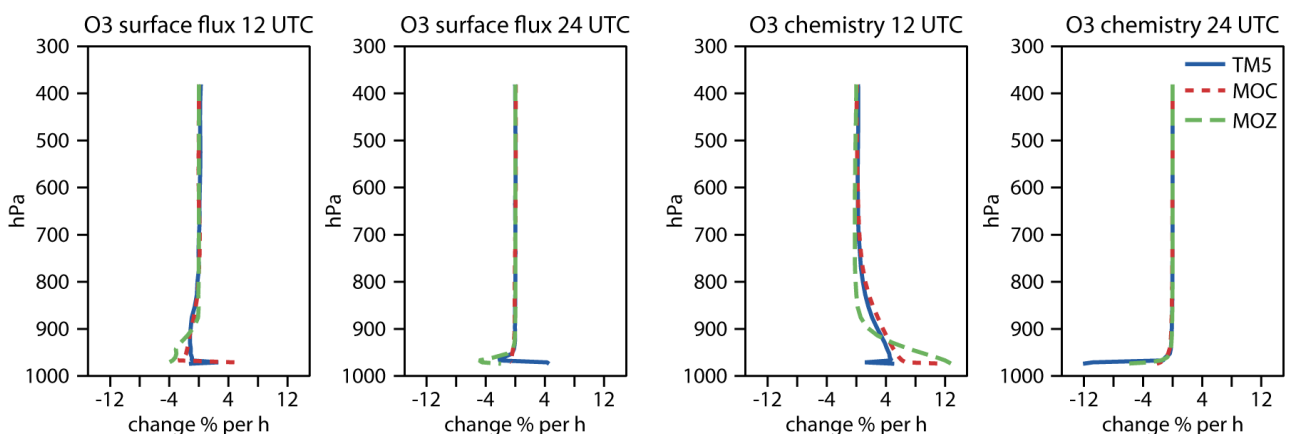


Figure 5 Profile of the area averaged (over Europe) relative changes per hour in percent of O<sub>3</sub> due to chemistry and due to deposition from TM5, MOZART-3 (MOZ) and MOCAGE (MOC) at 12 and 24 UTC.

## 4. Validation of the coupled system in near-real-time forecast mode for O<sub>3</sub> and CO

The performance of four-day forecasts of global reactive gases by the coupled system IFS-MOZART in near-real-time mode (NRT) for the period November 2007 to November 2008 is investigated in this section. Daily hindcast runs over 24 h with IFS-TM5 for the period September to November 2008 (SON) are also included in the evaluation. Since the PBL has been identified in Section 0 as the area where the coupled IFS and the CTM differ most, the model evaluation is based on surface observation of CO and O<sub>3</sub> from stations of the GAW surface network. Six stations from different parts of the globe contributed to the evaluation (see Table 3) of the near-real-time runs. The number of stations is small because of a delay in the availability of GAW data from other stations. Nevertheless, the wide-spread distribution of the six stations made it possible to draw valid conclusion of the model performance on a global scale. The stations Monte Cimone (MCI, Italy), Izana (IZO, Tenerife), Tamanrasset-Assekrem (TAM, Algeria) and Hohenpeissenberg (HPB, Germany) are mountain sites whereas Cape Point (CPT, South Africa) and Neumayer (NEU, Antarctica) are located in flatter terrain. There were no CO observations from all season and no O<sub>3</sub> observation for December 2007 to February 2008 (DJF) available from NEU. The IZO data set lacked observations from July to August 2008 (JJA) for both CO and O<sub>3</sub>. The location of the stations is shown in Figure 6

The coupled system IFS- MOZART-3 has been used to provide forecasts of atmospheric composition since May 2007. The results of the O<sub>3</sub> and CO forecast are published daily at the GEMS web-site <http://gems.ecmwf.int/d/products/grg/realtime/>. Beside providing a global picture of atmospheric composition, the results of the NRT forecast are used as boundary conditions for European regional air quality models run daily within the GEMS project.

The emission data used in the forecast are based on the year 2000 inventory from the RETRO project (<http://retro.enes.org>). Monthly averages of Global Fire Emission Database (Randerson et al., 2006) for the period 1997-2004 (MOZART-3) or 2001-2006 (TM5) were used as wild fire emissions. The meteorological initial conditions were obtained from ECMWF's operational high-resolution forecast. The initial concentration fields for MOZART-3 were taken from the previous 24 h forecast. The coupled system was run in "total tendency mode" without feedback.

### 4.1. Vertical representativeness of the GAW observation

An evaluation with surface observations of CO and O<sub>3</sub> needs to consider the representativeness of the data against the model resolution. Tilmes and Zimmermann (1998) and Flemming and Stern (2007) are examples of studies investigating horizontal representativeness which highlight the horizontal heterogeneity of air quality observations. The available GAW observations were considered to be suitable for evaluation of global model output with a horizontal resolution of about 125 km because they are located in areas without strong local emissions, and because obvious local effects have been removed from the data by the data providers. For example, Folini et al. (2009) specify a radius of influence for the station MCI of 339 km. Only the station Santa Cruz (Tenerife), which is located in the same grid box as IZO, was excluded because the standard deviation (SD) of the observed values was up to ten times higher than the modelled SD whereas for all other stations the modelled and observed standard deviation agreed within a +/- 50% margin.

Although the used stations seemed horizontally representative, attention had to be given to the vertical representativeness of the observations because many sites are located on mountains. The vertical resolution of the IFS and MOZART-3 in the coupled system covers the lowest 2 km with about 15 levels. Given the often pronounced vertical concentration gradients in the PBL, the selection of the corresponding model level was a critical issue. To quantify this sensitivity the mean modelled differences between the lowest model level (10 m) and the level at 1000 m above the model surface were calculated for the period SON. For the European stations MCI and HPB this vertical gradient was 88% and 70% of the observed CO value, whereas the vertical gradient was very small at IZO and TAM. A strong average vertical concentration gradient means that the choice of the modelled level used in the evaluation strongly influences the inferred model bias. Besides a different strength of the PBL mixing, the vicinity of stronger CO emissions in the respective model grid box could be the reason for the strong vertical gradient at MCI and HPB despite similar CO concentrations at all stations. The modelled mean O<sub>3</sub> levels decreased for all stations with height. The stations MCI and HPB showed again the largest differences of about 64% and 44% of the observed value.

The choice of the corresponding model level should reflect to what extent an observation samples air which is influenced by surface processes. The surface influence depends on the shape of the relief in the close vicinity of the observation site. In a first attempt, the model level corresponding to the measurement was chosen based on the difference between the station altitude and the height of the underlying model orography. However, when applying this procedure to the orography (125 km resolution) of the coupled system the altitude of HBP, which is an isolated mountain close to the Alps, was below the model orography. The reason for this was that the nearby Alps contributed to the average model orography in the respective grid box. Therefore orography data with a higher horizontal resolution of 50, 25 and 16 km (see Table 3) were also considered because they provided better guidance on the actual relief around the station. It was then decided to base the level choice on the 16 km orography, which differed only to a small extend from the 25 km orography. This meant that for the two most sensitive stations in terms of the vertical profile, HBP and MCI, the corresponding model level height changed from minus 118 m to 305 m and from 1940 to 1115 m respectively.

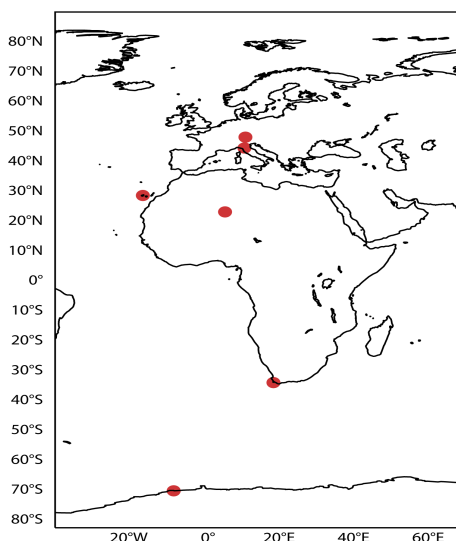


Figure 6 Location of the six GAW stations (see Table 3)

Table 3 Station location (lat, lon), altitude above sea level (asl), model level choice for the evaluation (LEV, 60 is lowest level) station height above orography with a resolution of 125 and 16 km, mean vertical gradient in the PBL expressed as modelled difference between surface and 1 km height divided by the observed mean for CO and O<sub>3</sub> over the period 1.9.2008 - 31.11.2008.

Name	Lat (°N)	Lon (°E)	Asl (m)	Lev	Height above orography (m)		Vertical PBL Gradient in (%)	
					125 km	16 km	CO	O <sub>3</sub>
CPT Cape Point	-34.4	18.5	230	56	78	230	26	-29
HPB Hohenpeißenberg	47.8	11	980	54	-118	305	70	-64
IZO Izana	28.3	-16.5	2376	50	2312	986	4	-5
MCI Monte Cimone	44.2	10.7	2169	50	1940	1115	88	-44
NEU Neumeyer	-70.6	-8.25	42	58	57	41	-	-27
TAM Tamanrasset-Assekrem	22.8	5.5	1377	50	1437	1420	1	-36

Finally, the match of temperature and relative humidity observations at HBP with simulated values was studied for the model levels in the PBL. This comparison should provide more insight into the representativeness of the selected model level. The simulated parameters at the chosen model level 54 agreed better overall with the observed variability than model levels above or below. However, only small differences between the temperature at level 54 and the lowest model level 60 were found whereas the simulated CO and O<sub>3</sub> concentration differed largely between the two levels because of the pronounced simulated diurnal concentration cycle at the surface. The observed day-to-day variability of the relative humidity was well captured by the model but no clear pattern could be identified to suggest which of the levels agreed best in terms of the diurnal cycle.

#### 4.2. Seasonal mean values

Figure 7 and Figure 8 show the observed and modelled CO and O<sub>3</sub> seasonal mean concentration derived from the first forecast day of the NRT run with IFS-MOZART for the periods DJF, March to May 2008 (MAM), JJA and SON as well as the season SON for IFS-TM5. The stations are displayed according to their latitude from North to South.

Observed and forecast CO show a similar gradient between the Northern and Southern Hemisphere. CO was on average overestimated by 10-20 ppb at the subtropical sites (CPT, IZO, TAM) and in JJA and SON at the European mountain site MCI by the coupled system IFS-MOZART. A general underestimation occurred at HPB, which was caused by a strong underestimation in the DJF and MAM season at HBP, whereas later in the year the forecast was nearly unbiased. The prediction at MCI was also too low in DJF and MAM. For both these European sites HBP and MCI, the measurements showed a pronounced maximum for both seasons, which was less developed in the modelled values. The general differences between the seasons were simulated correctly but the seasonal differences were smaller in the model result. The biases of IFS-TM5 for the SON season were similar to the ones of IFS-MOZ, i.e. no bias at HPB and an overestimation of about 20 ppb for the other sites.

The coupled system IFS-MOZART underestimated the mean  $O_3$  values everywhere apart from HPB. The typical negative bias was in the range of minus 5 to minus 10 ppb with exception of the Antarctic station NEU, where  $O_3$  values were underestimated by about 15-20 ppb which is about half of the observed value. The coupled system with TM5 simulated the average SON  $O_3$  values about 10 ppb higher than MOZART-3, leading to a positive bias at all stations apart from NEU. The higher values meant a smaller absolute bias for TM5 at NEU, CPT, IZO, MCI but also a bigger error at HBP and TAM. The higher  $O_3$  values in TM5 might be related to the lower  $O_3$  deposition and higher  $O_3$  chemical production above 900 hPa (see Figure 5) which was identified in Section 3.2. The observed  $O_3$  inter-annual variation for the considered period was about 10 ppb. The observed seasonal cycle showed a maximum mostly in MAM and JJA. Notable seems to be that the  $O_3$ -maximum also occurred in JJA at the two stations CPT and NEU in the Southern Hemisphere. Only TAM showed a maximum in the season DJF, however the seasonal cycle was not very pronounced at this site. The coupled system IFS-MOZART predicted the seasonal variability in a reasonable way but it exaggerated the JJA maximum at the European mountain sites HBP and MCI. The missing spring maximum could indicate an underestimation of the transport from the stratosphere to the PBL.

It is worthwhile to note that MOZART-3 has recently been updated to account for changes in reaction coefficients and undergone various small developments. The new version yields somewhat higher ozone values which should reduce the bias reported here.

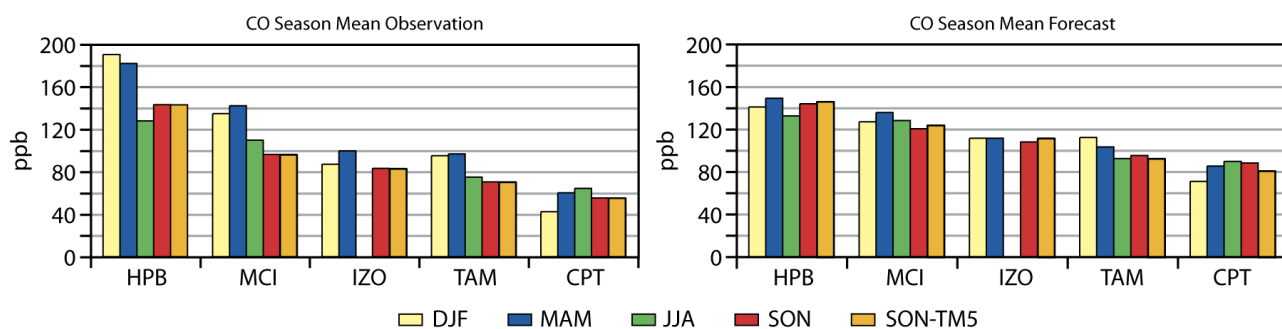


Figure 7 Observed (left) and modelled (right) CO mean concentration of the 1 day forecast for the seasons DJF, MAM, JJA and SON for six GAW stations with the coupled system IFS-MOZART, and for the season SON with the coupled system IFS-TM5 (SON-TM5)

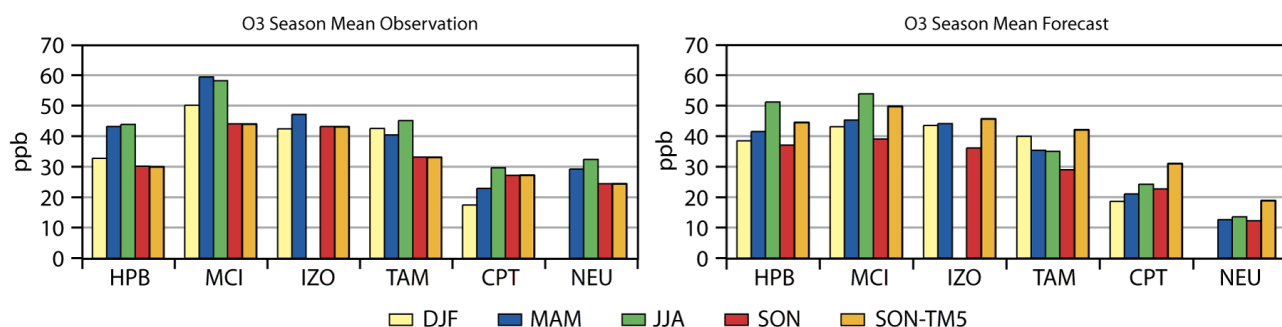


Figure 8 Observed and modelled  $O_3$  mean concentration of the 1 day forecast for the seasons DJF, MAM, JJA and SON for five GAW stations with the coupled system IFS-MOZART, and for the season SON with the coupled system IFS-TM5 (SON-TM5)

To find out if the dislocation between the CTM and the IFS (see Section 3.1) caused a change in the forecast accuracy, the CTM stand-alone output was also compared with the GAW observations. The RMSE of three-hourly data in the season SON (see Figure 9) was of very similar value for most of the stations, indicating no significant difference in the performance of the coupled system compared to the CTM stand-alone run. The largest differences occurred at the station CPT where O<sub>3</sub> was better simulated by the IFS in the coupled system and CO better by the stand-alone CTM. Figure 11 and Figure 12 show time series of the observation and the simulation of the coupled system and the MOZART-3 direct output. There was a minimal offset, small compared to the bias against the observations, between the coupled system and the direct CTM output, which caused a higher or lower RMSE for CO and O<sub>3</sub> respectively. The height of the peaks was higher in the coupled model output which seems to better match the observations. It was inferred that the differences between the IFS and CTM fields were mainly caused by the different horizontal grid partitioning in the IFS and the CTM, which attributes a different amount of emission in the grid box where the observation is located.

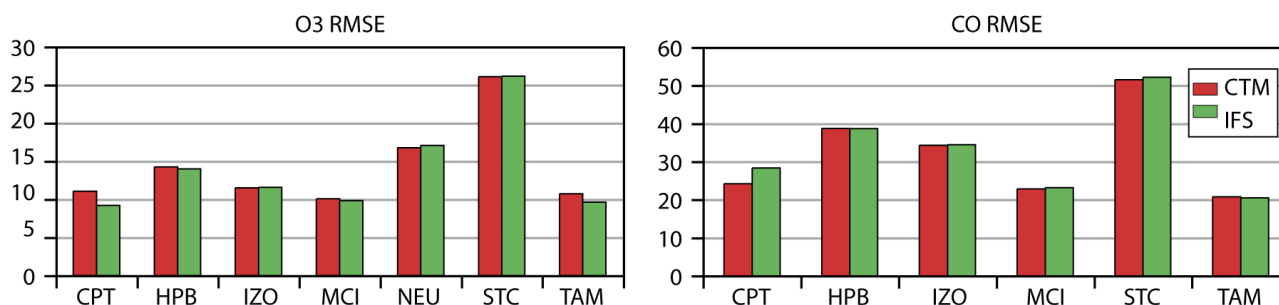


Figure 9 RMSE for CO (left) and O<sub>3</sub> (right) the season SON 2008 calculated from tracer fields of the IFS in the coupled system (IFS) and from direct MOZART-3 output (CTM) for six GAW stations.

### 4.3. Day-to-day variability

The bias of the forecast with respect to the observations is a consequence of the shortcomings in the CTMs emission data, chemical mechanism and physical parameterisations. In the case of surface observations as discussed in Section 4.1, the PBL mixing and the correct choice of the model level also play an important role. In contrast to the bias, the evaluation of day-to-day variability tests more the response of the model to changing local meteorological conditions and the long range transport. To quantify the day-to-day variability the standard deviation (SD) and correlation (COR, see Figure 10) of the daily mean values as well as the correlation of the linearly de-trended daily mean values was calculated for each season. The correlation of the de-trended data is equivalent to correlation of the concentration change from one day to the next day. Removing a trend before the calculation of the correlation is good statistical practise (Wilks, 2006) because it ensures the statistical stationarity of the time series.

For CO, observed and simulate SD agreed well, with the observed SD being about 10-30% higher than the modelled SD. Notable is that the observed SD was about twice as high as the corresponding model SD for HBP in DJF and SON and that these observed SDs were also two times higher than the observed SD at other locations in the same seasons. This could mean that this variability was caused by sub-scale processes such as local emission sources not resolved by the coupled system.

The correlation of the CO daily mean was in the range from 0.4 to 0.9 for all stations and seasons. The highest correlations were reached at CPT in the seasons SON and DJF. As shown in Figure 11, the observed individual CO peaks were well captured by the model. The highest observed and modelled CO values at CPT were associated with modelled winds coming from the North-West, and secondary maxima occurred with Easterly winds. The lowest correlation occurred at HPB when the variability of the observations strongly exceeded that of the model. De-trending of the data lead to a decrease of the correlation, which means that possible trends within a season were correctly simulated. For IZO in SON and HBP in DJF the de-trended COR was significantly below the trended COR which indicates the value of the latter was caused by a correct trend rather than a correct simulation of the day to day variability.

The SDs for O<sub>3</sub> were in the range of 3 to 10 ppb for all stations and seasons. The SD of the model exceeded that of the measurements at almost all stations in DJF and SON, whereas the observed SD was bigger than the model SD in the rest of the year. The higher modelled O<sub>3</sub> SD could indicate an overestimation of the PBL activity at the selected model level, or overestimated chemical activity.

With the exception of NEU in MAM, the COR of the CO daily average was between 0.35 to 0.8 for all stations and seasons. The negative correlation at NEU in MAM was caused by a small but missing positive trend in the model since COR of the de-trended data was 0.43. As with CO, COR values for O<sub>3</sub> higher than 0.7 could be achieved at CPT in all seasons apart from JJA, and in DJF and MAM at MCI and TAM.

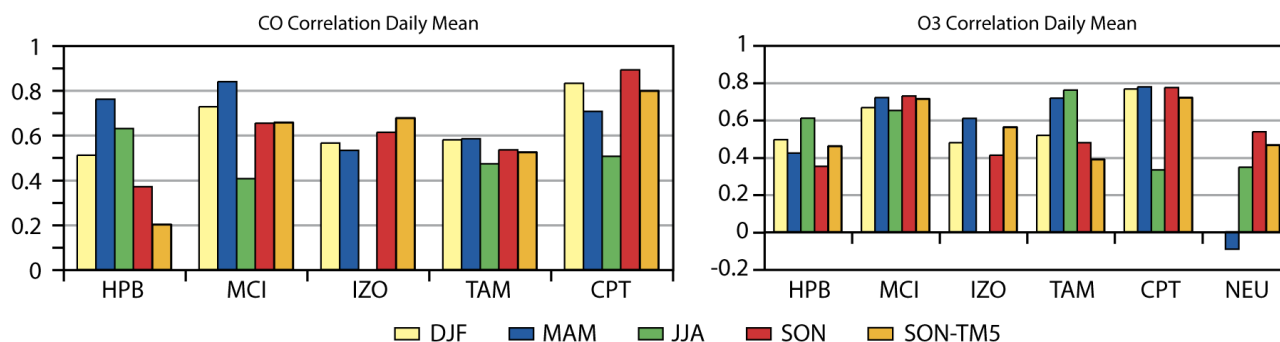


Figure 10 Correlation of the predicted and observed daily O<sub>3</sub> and CO mean of the 1 day forecast by IFS-MOZART (all Seasons) and IFS-TM5 (SON-TM5) for GAW stations.

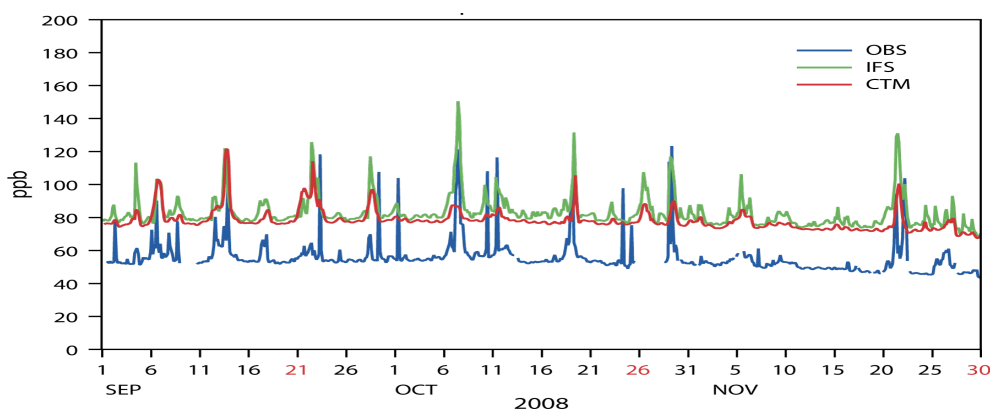


Figure 11 Time series of CO modelled by the IFS in the coupled system (IFS, green) and by the CTM MOZART-3 (MOZ, red) and observations (OBS, blue) for the GAW station Cape Point, which showed the largest differences in RMSE between IFS and CTM.

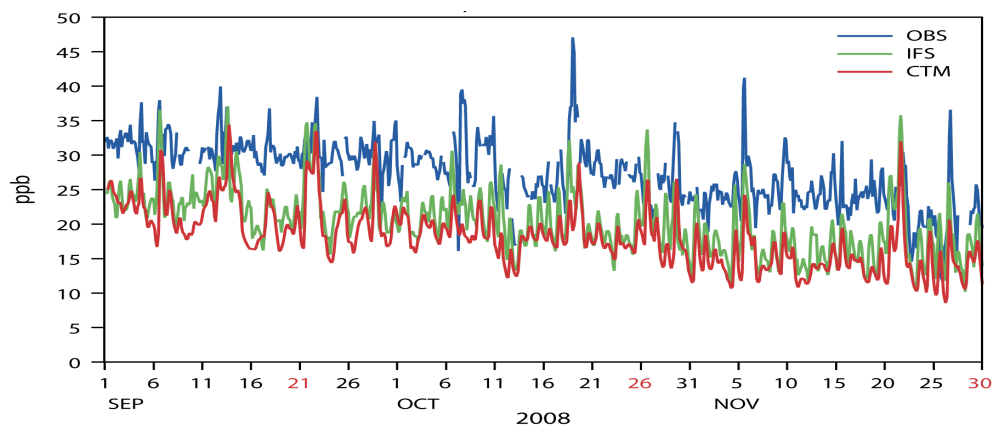


Figure 12 Time series of  $O_3$  modelled by the coupled system (IFS, green) and by the CTM (MOZ, red) and observations (OBS, blue) for the GAW station Cape Point, which showed the largest differences in RMSE between IFS and CTM.

#### 4.4. Predictability

The change in the accuracy of the forecast of the daily mean over the forecast period of four days is investigated in this section. In particular, the forecasts are compared to a persistency forecast as a reference to determine the skill of the forecast. The forecast quality could deteriorate with increasing forecast length (i) because of the increasing error of the meteorological forecast and (ii) because of an increasing dislocation (see Section 0) between the IFS concentration fields and the CTM tendency fields.

The persistency forecast assumes that the last observed daily mean is predicted for each forecast day. Hence, the persistency forecast is un-biased and its correlation is equivalent to the auto-correlation of the observations with a lag 1 to 4. Since the persistency forecast is un-biased and non-negligible biases of the forecast have been identified in Section 0, it seems more worthwhile to compare variability-evaluating measures such as RMSE and correlation against the persistency reference.

Bias, RMSE and correlation of the daily mean was calculated for each of the four forecast days in each seasons. A general finding was that not only the bias but also the other forecast quality parameters did not change largely over the forecast period. This fact indicates that the influence of the synoptic scale meteorological forecast error as well as the dislocation, which is specific to the coupled system, is small compared to the CTM-specific errors caused by emission data uncertainty, imperfection of the chemical mechanism and the PBL scheme and any un-resolved sub-grid scale variability.

The following discussion is limited to the period SON for the sake of brevity. Figure 13 shows the RMSE of the CO and  $O_3$  daily mean, based on 6 hourly values, for each forecast day. The CO RMSE remained nearly constant for all stations apart from MCI which showed an increase of about 20%. The  $O_3$  RMSE varied within about 10% for all stations. Since the bias contributes to the RMSE, only at locations with a small bias can the RMSE of the forecast be expected to be similar or lower than the RMSE of the persistency forecast. HBP showed the lowest bias for both CO and  $O_3$  in the season SON, and therefore the RMSE of the persistency forecast for this station was also included in Figure 13. The RMSE of the HBP persistency

forecast increases with increasing forecast length. The forecast with the coupled system for CO was already after the first forecast day better than the persistency forecast in respect to RMSE. For  $O_3$ , a RMSE similar to the reference was achieved at HPB at the fourth forecast day.

To dismiss the influence of the bias, the correlation of the forecast daily mean from the coupled system IFS-MOZART  $r_{IFS-CTM}$  and the correlation from the persistency forecast  $r_{Per}$  were compared by applying a skill score  $SS$ :

$$SS = \frac{r_{IFS-CTM} - r_{Per}}{1 - r_{Per}} \cdot 100\%$$

$SS$  relates the difference of the accuracy parameter of the forecast and the reference forecast to the difference between the accuracy parameter of the perfect forecast and the reference forecast (Wilks, 2006). A skill score greater than zero means that the forecast is better than the reference, and a skill score of one means a perfect model forecast.

As the correlation of the forecast of the daily mean  $r_{IFS-CTM}$  did not decrease much over the forecast period, the skill score of the forecast is mostly influenced by the drop in  $r_{Per}$ , i.e. the auto-correlation of the observed daily means with increasing lag, i.e. forecast day. A low auto-correlation at a certain lag indicates that most of the variability appears in time scales smaller than the given lag. For CO, the stations HPB and CPT showed the fastest drop in auto-correlation over the four days whereas for MIC and IZO the auto-correlation decreased much more slowly. For stations with little day-to-day O<sub>3</sub> variability such as NEU and CPT the auto-correlation only decreased slightly over the period, whereas for the mountain sites HBP and MCI almost no auto-correlation could be found already by the third forecast day.

Figure 14 shows the skill score of the correlation with respect to the persistency forecast for CO and O<sub>3</sub>. Positive skill scores were found for almost all stations on every forecast day, which means that the forecast of the coupled system provides useful information for the whole forecast period in terms of capturing the day to day variability. The highest skill score for CO of almost 0.8 was achieved at CPT because the small-scale daily variability could be resolved by the coupled system over the whole forecast period. A skill score of 0.6 at MCI was the highest value for O<sub>3</sub>. The quick drop in the auto-correlation for both CO and O<sub>3</sub> at HBP lead to a steady increase of the skill at this location.

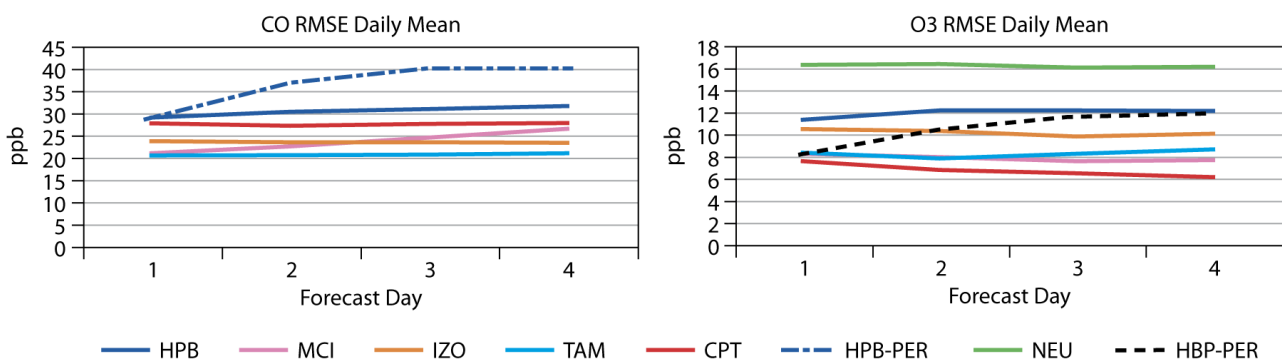


Figure 13 RMSE of the daily mean of CO (left) and O<sub>3</sub> (right) in the period 1.9.-30.11.2008 on the 1<sup>st</sup> to 4<sup>th</sup> forecast day at six GAW Stations and additionally for the persistency forecast at Hohenpeißenberg (HBP-PER)

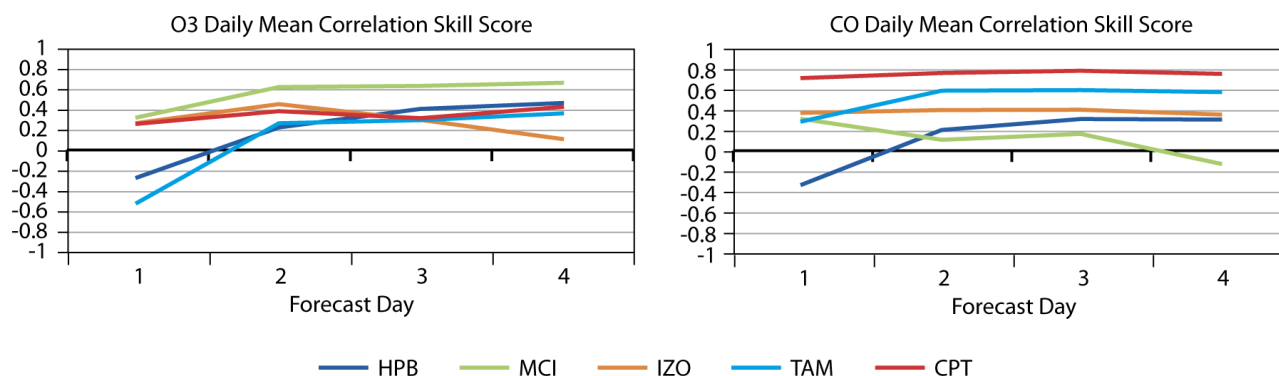


Figure 14 Skill Score in respect to persistency forecast for the correlation of the daily mean for CO (left) and O<sub>3</sub> (right) on the on the 1<sup>st</sup> to 4<sup>th</sup> forecast day at six GAW Stations. A positive skill score means that the model forecast is better than the persistency forecast, negative values indicate a better persistency forecast.

## 5. Summary and Conclusion

The design and the validation of a coupled system which links the ECMWF's Integrated Forecast and data assimilation System (IFS) to each of the three global CTMs, MOZART-3, TM5 and MOCAGE, are presented in this paper. The purpose of the coupled system is to enable the IFS to simulate global reactive gases in order to provide forecasts and analyses of atmospheric composition without directly integrating complex chemistry schemes, emission injection and deposition into the IFS. The coupled system is an alternative approach to the on-line integration of chemistry-schemes in meteorological models. The main motivation for developing the coupled system was the ease with which different chemical schemes could be tested, and the reduced development effort. The coupled system IFS-CTM can directly utilise the IFS 4D-VAR algorithm to assimilate observations of atmospheric trace gases such as CO, tropospheric and stratospheric O<sub>3</sub>, SO<sub>2</sub>, NO<sub>x</sub> and HCHO. This paper focuses on the ability of the coupled IFS to simulate sound concentration fields by comparing them to (i) the concentration fields of the coupled CTM, which they should closely resemble and (ii) by comparing them to surface CO and O<sub>3</sub> observations of the GAW network.

In the coupled system, the CTM is driven by the meteorological data received from the IFS. The special characteristic of the coupled system is that the IFS receives either three-dimensional tendencies accounting for all source and sink processes or three-dimensional tendencies due to chemistry and net surface fluxes accounting for emission and dry deposition. The respective tendencies and fluxes are applied to the IFS concentration fields, whose transport has is modelled by the IFS.

To prove the validity of the coupled approach, the chemical tracers in the coupled system IFS-MOZART were compared with concentration fields from MOZART-3. Only small differences were found for a period of about 48 hours. The largest differences occurred in the PBL. A comparison with observations from the GAW network showed that these small differences lead to sometimes slightly bigger and sometimes smaller errors with respect to observations.

The exchange of tendencies describing emission injection and deposition as well as chemical conversion is a special feature of the coupled system. The tendencies were used for a process-oriented inter-comparison of the three CTMs, MOZART-3, TM5 and MOCAGE, over Europe in June 2004. Averaged profiles for day and night conditions showing the impact of the surface fluxes (i.e. emissions, deposition, diffusion) were compared with profiles showing the impact of the chemical conversion.  $\text{NO}_x$  was the most variable species with average changes per hour of up to 30% of the concentration value for both chemistry and emission injection. The maximum relative  $\text{O}_3$  changes were due to chemistry and reached up to 5% in the PBL. Emissions of CO caused an increase of up to 3% and its chemical depletion was up to 1% of the concentration value per hour. Even with such a large variability,  $\text{NO}_x$  could be reasonably well simulated with the coupled system. Despite the surface emission, diffusion caused a net loss close to the surface and an accumulation in the upper part of the PBL in all CTMs during the day. The day-time vertical mixing was shallowest in MOZART-3. The chemical loss of CO and  $\text{NO}_x$  linked to the reaction with the hydroxyl radical was highest in MOCAGE. In contrast MOCAGE's night time  $\text{NO}_x$  depletion was much lower than that of the other two CTMs, with TM5 simulating the largest chemical  $\text{NO}_x$  loss. MOCAGE's dry deposition of  $\text{O}_3$  was confined to the lowest model layer and was stronger than in the other CTMs.

The coupled system IFS-MOZART has been used to forecast global atmospheric composition since May 2007. Additionally, one-day runs with the coupled system IFS-TM5 were carried out for the season September to November (SON) 2008. The forecasts were compared with observational data from GAW stations in Europe (Hohenpeißenberg and Monte Cimone), Africa (Izana, Tamanrasset-Assekrem and Cape Point) and the Antarctic (Neumeyer Station) for each season from December 2007 to November 2008.

Although the horizontal representativeness of these stations seemed large enough for a meaningful comparison with model result of about 125 km horizontal resolution, the vertical representativeness, i.e. the choice of the corresponding model level had great influence on the obtained bias and diurnal cycle because of the sometimes large modelled vertical gradient. A high average modelled vertical gradient was noticed over the lowest 1000 m at Hohenpeißenberg and Monte Cimone. The modelled vertical difference was up to 88% of the observed value for CO and up to minus 64% for  $\text{O}_3$ . MOZART-3 may tend to overestimate the vertical gradient because TM5 and MOCAGE showed a more mixed PBL, but gradients of up to 50% were also found in the other two models. The large vertical gradient means a difference in model level choice by one level could already introduce an additional relative bias of 8% in the case of MOZART-3. It was decided to base the important choice of the model level corresponding to the observation on the difference between the station altitude and a high resolution (16 km) orography.

In the NRT forecast, IFS-MOZART mostly underestimated  $\text{O}_3$  by 5-10 ppb; the largest negative bias of about 15 ppb occurred at Neumeyer station. IFS-TM5 values for the period SON were about 10 ppb higher than the ones from MOZART-3 causing a small overestimation everywhere apart from the Antarctic. CO was mostly overestimated by up to 20 ppb by both IFS-MOZART and IFS-TM5. The hemispheric CO gradient was correctly captured. The differences between the seasons, i.e. the inter-annual variation as well as the standard deviation of the model and the observations agreed reasonably well for both  $\text{O}_3$  and CO.

The forecast performance measured in terms of bias, RMSE and correlation of daily mean values changed only very little over the forecast period of four days. It could therefore be concluded that neither the increasing meteorological forecast error nor the increasing dislocation between the coupled IFS tracers and the CTM tendencies influenced the achieved model performance to a large extent. This means that the synoptic-scale forecast after four days is still good enough to simulate the transport processes. It further proves the validity of the coupled approach - at least for CO and O<sub>3</sub> - for a forecast length of up to four days.

The correlation of daily mean values was in the range of 0.4-0.9 for CO and 0.3-0.8 for O<sub>3</sub> within each season. The best correlation could be achieved for Cape Point where individual CO spikes linked to forecast north-westerly winds were very well reproduced by the coupled system.

The forecast skill score in respect to the “persistence” forecast was evaluated for the season SON. The persistence forecast is unbiased and its correlation is the autocorrelation of observations. Only for CO at Hohenpeißenberg after the first days could an RMSE be found, which was lower than the persistence reference. However, a positive skill score in terms of correlation occurred from day two onwards at almost all stations for both CO and O<sub>3</sub>. This proved that the four day forecast with coupled system provided meaningful results in terms of the day-to-day variability over the whole forecast of four days.

In summary, the IFS tracer fields of the coupled system compared well with the corresponding CTM fields and with CO and O<sub>3</sub> observations. It can be concluded that the coupled system is a flexible and scientifically sound instrument for the forecast of atmospheric composition. These are important pre-requisites for its use in the assimilation of satellite observation of reactive trace gases, which has already been demonstrated by Inness et al. 2009. The coupled system further provides valuable insight for process-oriented model evaluation because of its direct access to contribution of source and sink processes.

Data products (reanalyses and forecasts) from the coupled IFS-MOZART model are available routinely on <http://gems.ecmwf.int>.

## Acknowledgments

We thank the operators of the Global Atmosphere Watch stations Hohenpeißenberg, Monte Cimone, Izana, Santa Cruz, Tamanrasset-Assekrem, Cape Point and Neumeyer station for the timely provision of their observational data. We would like to acknowledge Rene Redler’s and Sophie Valcke’s support during the implementation of the OASIS4 coupler software, and Lukes Jones for proofreading the text. The work has been carried out in the GEMS project, which is funded by the European Commission under the EU Sixth Research Framework Programme, contract number SIP4-CT-2004-516099. Finally, we would like to acknowledge Tony Hollingsworth who sadly passed away in summer 2007 for his enthusiastic support and for being the first to sketch out the design of the coupled system.

## References

- Bechtold, P., Bazile, E., Guichard, F., Mascart, P., and Richard, E.: A mass flux convection scheme for regional and global models, *Q. J. Roy. Meteor. Soc.*, 127, 869-886, 2001.
- Beljaars, A., Bechtold, P., Kohler, M., Morcrette, J-J., Tompkins, A., Viterbo, P. and Wedi, N.: The numerics of physical parameterization, Seminar on Recent developments in numerical methods for atmospheric and ocean modelling, 6-10 September, 2004. (<http://www.ecmwf.int/publications/>)

- Bousserez, N., Attié, J.-L., Peuch, V.-H., Michou, M., and Pfister, G.: Evaluation of the MOCAGE chemistry and transport model during the ICARTT/ITOP experiment, *J. Geophys. Res.*, 112, D10S42, doi:10.1029/2006JD007595, 2007.
- Cariolle, D. and Deque, M.: Southern hemisphere medium-scale waves and total ozone disturbances in a spectral general circulation model, *J. Geophys. Res.*, 91D, 10825–10846, 1986.
- Carslaw, K. S., Luo, B., Peter, T., and Clegg, S. L.: Vapour pressures of H<sub>2</sub>SO<sub>4</sub>/HNO<sub>3</sub>/HBr/H<sub>2</sub>O solutions to low stratospheric temperatures, *Geophys. Res. Lett.*, 22, 247-250, 1995.
- Dethof, A. and Hólm, E.V: Ozone assimilation in the ERA-40 reanalysis project, *Quart. J. Roy. Met. Soc.* 130 pp.2851- 2872, 2004.
- Engelen, R. J., Serrar, S. and Chevallier, F.: Four-dimensional data assimilation of atmospheric CO<sub>2</sub> using AIRS observations, *J. Geophys. Res.*, 114, D03303, doi:10.1029/2008JD010739, 2009.
- Emmons, L. et al., Sensitivity of chemical tracers to meteorology in MOZART-4, in preparation
- Flemming, J and Stern, R.: Testing model accuracy measures according to the EU directives - examples using the chemical transport model REM-CALGRID, *Atmospheric Environment*, 41, 39, 206-9216, 2007.
- Folini, D., Kaufmann, P., Ubl, S. and Henne, S.: Region of influence of 13 remote European measurement sites based on modeled carbon monoxide mixing ratios, *J. Geophys. Res.*, Vol. 114, D8, D08307, 2009.
- Fortuin, J.P.F. and Kelder, H.: An ozone climatology based on ozonesonde and satellite measurements, *J. Geophys. Res.*, 103, 31709–31734, 1998.
- Ford, R. W. and Riley G. D: FLUME coupling review, UK Met-Office  
[http://www.metoffice.gov.uk/research/interproj/flume/pdf/d3\\_r8.pdf](http://www.metoffice.gov.uk/research/interproj/flume/pdf/d3_r8.pdf), 2002.
- Geer, A. J., Lahoz, W. A., Jackson, D. R., Cariolle, D. and McCormack, J. P.: Evaluation of linear ozone photochemistry parametrizations in a stratosphere-troposphere data assimilation system, *Atmos. Chem. Phys.*, 7, 939-959, 2007.
- Grell, G. A., Peckham, S. E. , Schmitz, R , McKeen, S. A., Frost, G. J, Skamarock, W. and Eder B.: Fully coupled online chemistry within the WRF model, *Atmospheric Environment* , 39, 37, 6957-6975, 2005.
- Hack, J. J.: Parameterization of moist convection in the NCAR community climate model (CCM2), *J. Geophys. Res.*, 99, 5551-5568, 1994.
- Hollingsworth, A., Engelen, R.J., Textor, C., Benedetti, A., Boucher, O. , Chevallier, F., Dethof, A., Elbern, H., Eskes, H., Flemming, J., Granier, C., Kaiser, J.W. , Morcrette, J.-J., Rayner, P., Peuch, V.H., Rouil, L., Schultz, M.G., Simmons, A.J and The GEMS Consortium: Toward a Monitoring and Forecasting System For Atmospheric Composition: The GEMS Project. *Bull. Amer. Meteor. Soc.*, 89, 1147-1164, 2008.
- Hólm, E. V., Untch, A., Simmons, A., Saunders, R., Bouttier, F. and Andersson, E.: Multivariate ozone assimilation in four-dimensional data assimilation. Pp. 89-94 in *Proceedings of the SODA Workshop on Chemical Data Assimilation*, 9-10 December 1998, KNMI, De Bilt, The Netherlands, 1999.
- Holtslag A.A. and Moeng, C.-H: Eddy diffusivity and counter-gradient transport in the convective atmospheric boundary layer. *J. Atm. Sci*, 48,1690-1698, 1991.

- Holtslag, A.A. and B. Boville: Local versus nonlocal boundary-layer diffusion in a global climate model, *J. Clim.*, 6, 1825-1842, 1993.
- Hortal, M. and Simmons, A. J.: Use of reduced Gaussian grids in spectral models, *Mon. Weather Rev.*, 119, 1057-1074, 1991.
- Houweling, S., Dentener, F., and Lelieveld, J.: The impact of non-methane hydrocarbon compounds on tropospheric photochemistry. *J. Geophys. Res.*, 103(D9), 10673-10696, 1998.
- Inness, A., Flemming, J., Suttie M. and Jones, L.: GEMS data assimilation system for chemically reactive gases, Technical Memorandum No. 587, European Centre for Medium-Range Weather Forecasts (ECMWF), 2009.
- Josse B., Simon P. and Peuch, V.-H.: Rn-222 global simulations with the multiscale CTM MOCAGE, *Tellus*, 56B, 339-356, 2004.
- Kaminski, J. W., Neary, L., Struzewska, J., McConnell, J. C., Lupu, A., Jarosz, J., Toyota, K., Gong, S. L., Côté, J., Liu, X., Chance, K., and Richter, A.: GEM-AQ, an on-line global multiscale chemical weather modelling system: model description and evaluation of gas phase chemistry processes, *Atmos. Chem. Phys.*, 8, 3255-3281, 2008.
- Kinnison, D. E., Brasseur, G. P., Walters, S., Garcia, R. R., Marsh, D. R., Sassi, F., Harvey, V. L., Randall, C. E., Emmons, L., Lamarque, J. F., Hess, P., Orlando, J. J., Tie, X. X., Randel, W., Pan, L. L., Gettelman, A., Granier, C., Diehl, T., Niemeier, U. and Simmons, A. J.: Sensitivity of Chemical Tracers to Meteorological Parameters in the MOZART-3 Chemical Transport Model. *J. Geophys. Res.*, 112, D03303, doi:10.1029/2008JD010739, 2007.
- Krol, M.C., Houweling, S., Bregman, B., van den Broek, M., Segers, A., van Velthoven, P., Peters, W., Dentener F. and Bergamaschi, P.: The two-way nested global chemistry-transport zoom model TM5: algorithm and applications *Atmos. Chem. Phys.*, 5, 417-432, 2005.
- Lefèvre, F., Brasseur, G. P., Folkins, I., Smith, A. K., and Simon, P.: Chemistry of the 1991-1992 stratospheric winter: three dimensional model simulations, *J. Geophys. Res.*, 99, 8183-8195, 1994.
- Lin, S. J., and Rood, R. B.: A fast flux form semi-Lagrangian transport scheme on the sphere, *Mon. Weather Rev.*, 124, 2046-2070, 1996.
- Louis, J.-F.: A parametric model of vertical eddy-fluxes in the atmosphere, *Bound. Lay. Meteor.*, 17, 187-202, 1979.
- Massart, S., Cariolle, D., and Peuch, V.-H.: Towards an improvement of the atmospheric ozone distribution and variability by assimilation of satellite data, *C. R. Geosciences*, 15, 1305-1310, 2005.
- Ménard, R. et al. ,Coupled chemical-dynamical data assimilation, Final Report, ESA/ESTEC. 2007.
- Morcrette, J.-J., Boucher, O., Jones, L., Salmond, D., Bechtold, P., Beljaars, A., Benedetti, A., Bonet, A., Kaiser, J. W., Razinger, M., Schulz, M., Serrar, S., Simmons, A. J., Sofiev, M., Suttie, M., Tompkins, A. M. and Untch, A.: Aerosol analysis and forecast in the ECMWF Integrated Forecast System. Part I: Forward modelling, *J. Geophys. Res.*, 2009.
- Mari, C., Jacob, D. J., and Bechtold, P.: Transport and scavenging of soluble gases in a deep convective cloud, *J. Geophys. Res.*, 105, 22 255-22 267, 2000.

- Pozzoli L., Bey, I., Rast, J. S., Schultz, M. G., Stier, P., and Feichter, J.: Trace gas and aerosol interactions in the fully coupled model of aerosol-chemistry-climate ECHAM5-HAMMOZ, PART I: Model description and insights from the spring 2001 TRACE-P experiment, *J. Geophys. Res.*, 113, 2008.
- Randerson, J. T., van der Werf, G. R., Giglio, L., Collatz, G. J. and Kasibhatla, P. S.: Global Fire Emissions Database, Version 2 (GFEDv2). Data set. Available on-line [<http://daac.ornl.gov/>] from Oak Ridge National Laboratory Distributed Active Archive Center, Oak Ridge, Tennessee, U.S.A. doi:10.3334/ORNLDAAC/834, 2006.
- Rast, S., Schultz, M.G., Bey, I., van Noije, T., Aghedo, A.M., Brasseur, G.P., Diehl, T., Esch, M., Ganzeveld, L., Kirchner, I., Kornbluh, L., Rhodin, A., Röckner, E., Schmidt, H., Schröder, S., Schulzweida, U., Stier, P., Thomas, K., Walters, S.: Interannual variability in tropospheric ozone over the 1980-2000 period: Results from the tropospheric chemistry general circulation model ECHAM5-MOZ, submitted to *J. Geophys. Res.*, November 26, 2008.
- Russell G.L. and Lerner. J. A.: A new finite-differencing scheme for the tracer transport equation. *J. Appl. Meteorol.*, 20:1483-1498, 1981.
- Sander, S.P., et al., Chemical Kinetics and Photochemical Data for Use in Atmospheric Studies, Evaluation Number 14, JPL Publication 02-25, Jet Propulsion Laboratory, Pasadena, Calif., 2003.
- Sander, S.P., et al., Chemical Kinetics and Photochemical Data for Use in Atmospheric Studies, Evaluation Number 15, JPL Publication 06-02, Jet Propulsion Laboratory, Pasadena, Calif., 2006.
- Schultz, M.G., Pulles, T., Brand, R., van het Bolscher, M. and Dalsøren, S. B.: A global data set of anthropogenic CO, NO<sub>x</sub>, and NMVOC emissions for 1960-2000, data available from [http://retro.enes.org/data\\_emissions.shtml](http://retro.enes.org/data_emissions.shtml), 2009.
- Singh, H., B. and Jacob, D.: Future directions: Satellite observations of tropospheric chemistry, *Atmospheric Environment* V34, 25, p 4399-4401, 2000.
- Tiedtke, M. A: comprehensive mass flux scheme for cumulus parameterization in large-scale models. *Mon. Weather. Rev.*, 117(8):1779-1800, 1989.
- Tilmes, S., and Zimmermann J.: Investigation on the spatial scales of the variability in measured near-ground ozone mixing ratios, *Geophys. Res. Lett.*, 25 (20), 3827-3830, 1998.
- Valcke S. and Redler R: OASIS4 User Guide (OASIS4\_0\_2). PRISM Support Initiative Report, No4, 2006.
- Van der Werf, G.R., Randerson, J.T., Giglio, L., Collatz, G.J. and Kasibhatla., P.S.: Interannual variability in global biomass burning emission from 1997 to 2004. *Atmos. Chem. Phys.*, 6, 3423 - 3441, 2006.
- Williamson, D. L. and Rash, P. J.: Two-dimensional semi lagrangian transport with shape-preserving interpolation, *Mon. Weather Rev.*, 117, 102-129, 1989.
- Wilks, D.S.: *Statistical Methods in the Atmospheric Sciences*, 2nd Ed. International Geophysics Series, Vol. 59, Academic Press, 627 p., 2006.
- Zhang, G. J., and N. A. McFarlane: Sensitivity of climate simulations to the parameterization of cumulus convection in the Canadian climate centre general circulation model, *Atmos. Ocean*, 33, 407-446, 1995.
- Zhang, Y.: On-line coupled meteorology and chemistry models: history, current status, and outlook, *Atmos. Chem. Phys*, 8, 2895-2932, 2008.